Bulletin of the Seismological Society of America, Vol. 71, No. 1, pp. 117–125, February 1981

WAVE SCATTERING FROM A STEP CHANGE IN SURFACE TOPOGRAPHY

By David M. Boore, Stephen C. Harmsen, and Sam T. Harding

ABSTRACT

Scattering of body waves to surface waves is a means for converting energy with essentially infinite horizontal wavelength to motion with short wavelengths. This process, of interest to engineers designing structures with large horizontal dimensions such as pipelines, tunnels, and bridges, has received little attention from seismologists. Finite-difference calculations have been performed for the simple case of vertically incident *SV* and *P* waves impinging on a step change in surface elevation. These calculations predict scattered Rayleigh waves with amplitudes as large as 0.4 times the amplitude of the surface motion of the incident waves in the absence of any topographic relief, even for incident wavelengths several times the height of the step. Both vertical and inclined steps are examined.

Introduction

The scattering of waves by imperfections in elasticity or by changes in the shapes of interfaces has been studied by many workers for a variety of reasons and by a number of methods. In this paper, we use finite-difference solutions to the wave equation to study the scattering of vertically incident P and S waves from a step change in surface topography. The motivation for this study comes from earthquake engineering, where there is concern that present design procedures may be inadequate if the ground motion contains horizontal wavelengths comparable to the size of a structure. For most structures, waves of relatively high frequency (e.g., 10 Hz) traveling with low apparent horizontal velocities (less than 1 km/sec) are needed to produce wavelengths short enough to be of concern (less than or equal to 100 meters). It is likely that such waves excited near the source will be insignificant because of scattering and anelastic energy absorption in traveling to the receiver.

A possible way of obtaining short horizontal wavelengths of significant amplitude is by the scattering of high frequency body waves into energy traveling essentially horizontally (e.g., coupling into surface waves). Previous workers have considered scattering of body waves by slots and canyons (e.g., Ilan *et al.*, 1979; Hudson and Boore, 1980) and by wedges of varying angle (e.g., Alterman and Loewenthal, 1970; Gangi and Wesson, 1978). This study differs from earlier work in that we have considered scattering of both P and S waves from a step change in surface topography (a slot or a mesa is made up of two steps of opposite sense); we also differ by concentrating on the scattered field and by considering the scattering in both the time and frequency domains. Although we were motivated by a problem in earthquake engineering, our results are useful in studies of signal-generated noise (Key, 1967, 1968; Greenfield, 1971) and in nondestructive materials testing (Bond, 1979). They also provide bench marks for comparison with laboratory experiments or approximate methods.

Method

A schematic representation of the problem is shown in Figure 1: a plane P or S wave propagates in a uniform, linear-elastic material (with Poisson's ratio of 0.22)

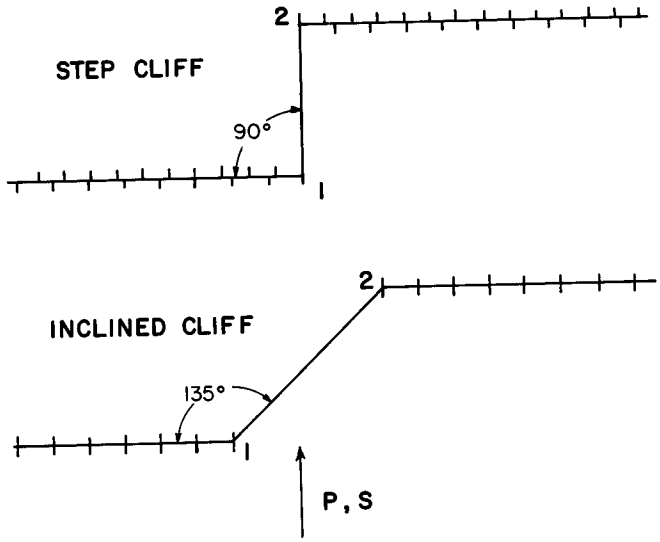

FIG. 1. (*Top*) Vertical step. Tick marks indicate locations where time histories were taken, *upper* ticks for *P* source, *lower* for *S*. The lower and upper corners are referred to elsewhere by the labels 1 and 2, respectively. The step was 17 and 29 grid spacings high for the incident *S* and *P* cases, respectively. (*Bottom*) Inclined step. Time histories for both *P* and *S* sources were taken at the tick marks. The vertical offset of the step was equal to 17 grid spacings.

TABLE 1

REFERENCE TO ALGORITHMS

Part of Model	Equations Used
Interior points	Alterman and Rotenberg (1969)
Corner points	Fuyuki and Matsumoto (1980); equations (13), (14), (15)*
Horizontal free surface	Ilan *et al.* (1975): equations (4.11), (4.12)
Vertical free surface	Ilan *et al.* (1975): equation (4.12a)
Inclined free surface	Ilan *et al.* (1975): equation (11) and Ilan and Loewenthal (1976): equation (24)
Side boundaries	Reflection symmetry (for vertical incidence)
Bottom boundary	Absorbing condition, Clayton and Engquist (1977)
Incident wave time-function	
(a) vertical step:	Boore (1972): equation (22)
(b) inclined step:	Ilan *et al.* (1979): equation (4)

* The *P* source models, run before we were aware of Fuyuki and Matsumoto (1980), used equations (4.26)–(4.28) of Ilan *et al.* (1975), but required a fine mesh to avoid ringing near the corner point. Fuyuki and Matsumoto's difference equations for the corners are more accurate, and a fine mesh is not required to eliminate the ringing.

toward a free surface with a vertical or inclined step change in topography. We have chosen a 45°-angle of incline. The problem is one of plane strain. Although the computer program allows an arbitrary angle of incidence, we consider only vertical incidence in this paper. Other angles give a more complicated but equally strong scattered wave field. Standard finite-difference algorithms were used to propagate the waves (Table 1). The motions at a number of points along the free surface were stored for later analysis. Snapshot displays (e.g., Boore, 1972) were formed but added little to the analysis here and are not displayed.

To emphasize the scattered waves, the motions that would have been recorded along a surface without any topographic relief (the reference motion) were subtracted from the compiled motions, and the resulting time series displayed in

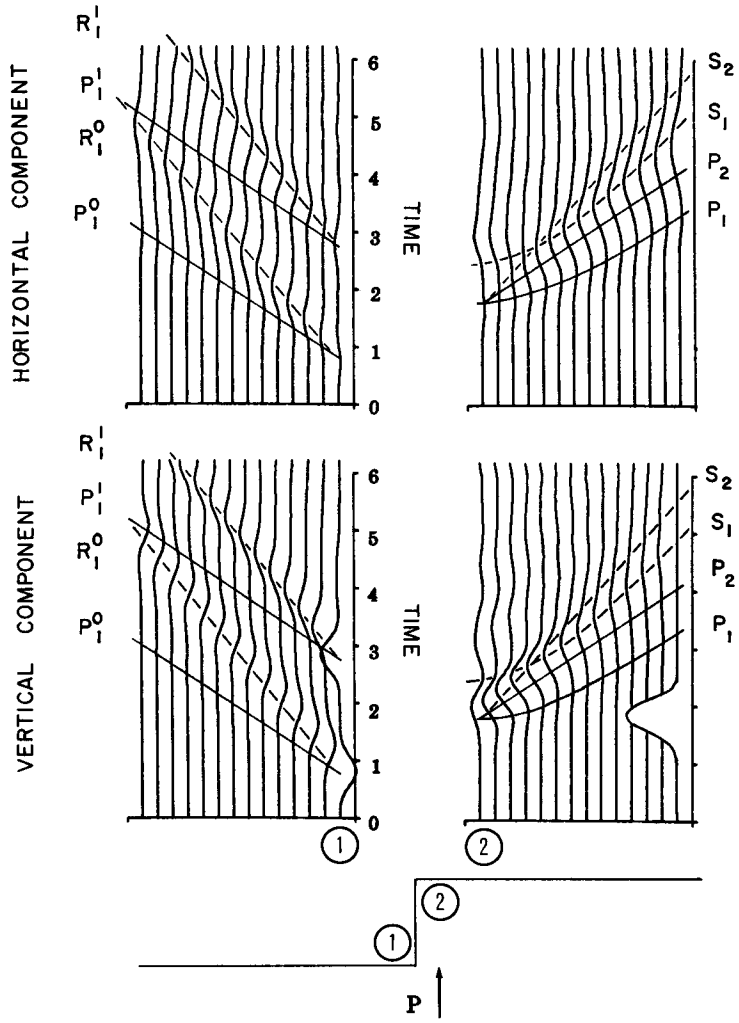

FIG. 2. Vertical step, P incident: scattered field time histories. Time is in dimensionless units, ct/h, where c = incident wave velocity, t = real time, and h = cliff height. Theoretical arrival times of important phases as plotted. Subscript refers to corner from which wave was scattered, superscript to scattering of incident (0) or reflected (1) wave. The reference motion is included in the rightmost vertical trace for comparisons. In this and subsequent figures, the cliff height and horizontal spacing between seismograms is to scale. As shown by circled numbers, innermost seismograms were recorded at vertices of step; the remaining traces were recorded at equi-spaced intervals along the upper and lower horizontal surfaces.

conventional time-distance sections, with the time scale normalized by the time taken by the incident wave to traverse the step height. Spectra of the scattered field, normalized by the spectra of the reference motions, were plotted with an abscissa equal to the wavelength of the incident wave divided by step height (cT/h, where c = velocity of incident wave, T = period, h = step height). The algorithms were checked against the results in Bouchon (1973), who used a different method to calculate the motions on the flank of a hill produced by incident plane waves. The agreement was excellent.

Results

Vertical step. Time series for incident P and S waves are shown in Figures 2 and 3, respectively. The reference motion is shown, for comparison, in the rightmost trace. To facilitate comparison, all seismograms are plotted to the same scale, even though this means losing detail for some of the scattered field. Superposed on the time series are theoretical travel-time curves for waves scattered at the two corners of the step (1, 2) by the incident (0) or reflected (1) wave. The source duration was short enough to allow easy identification of the scattered waves.

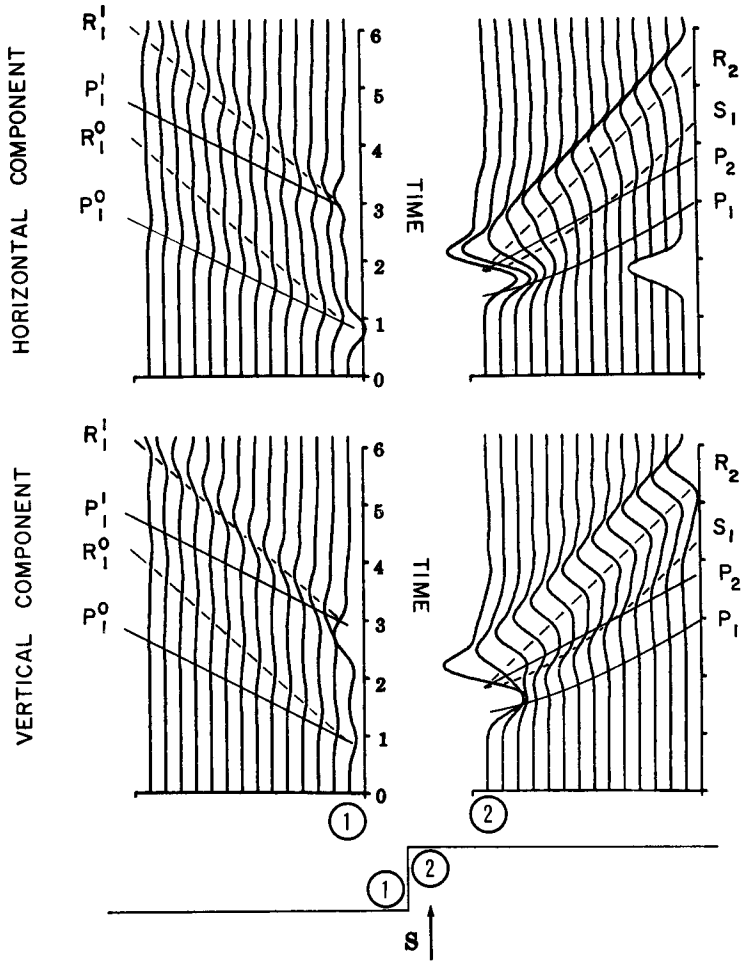

FIG. 3. Vertical step, S incident: scattered field time histories, with the reference motion added to the rightmost horizontal trace. See Figure 2 legend for additional details.

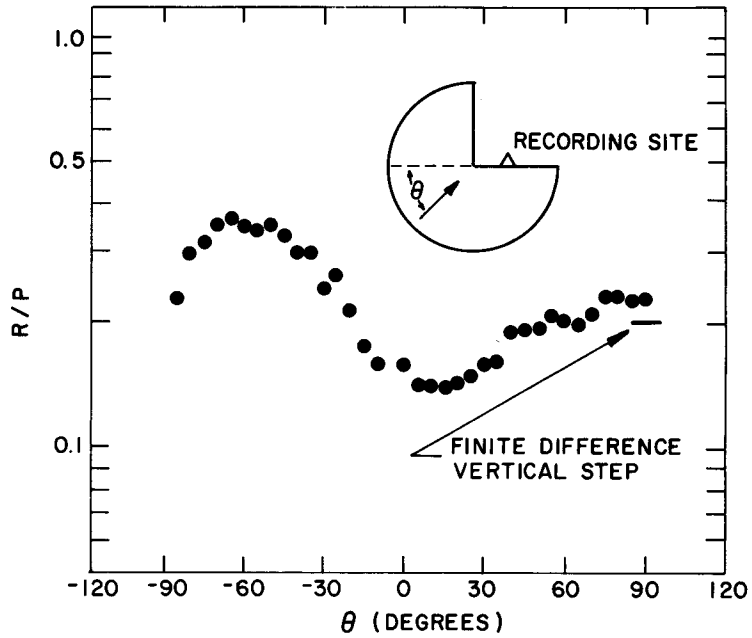

FIG. 4. Amplitude of Rayleigh wave at recording site normalized by P wave at corner, as a function of angle of incidence (Gangi and Wesson, 1978) and finite-difference result for vertical incidence.

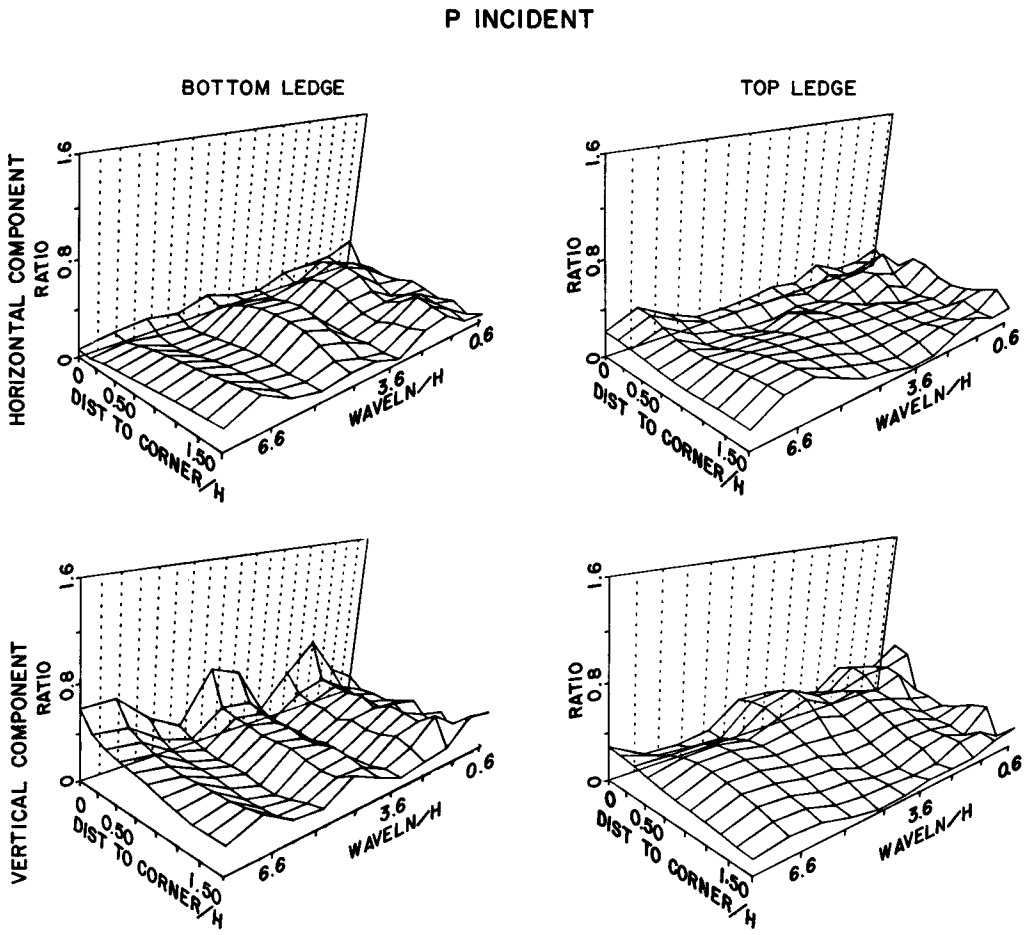

FIG. 5. Ratios of spectral amplitudes of scattered field and source for P incident on a vertical step.

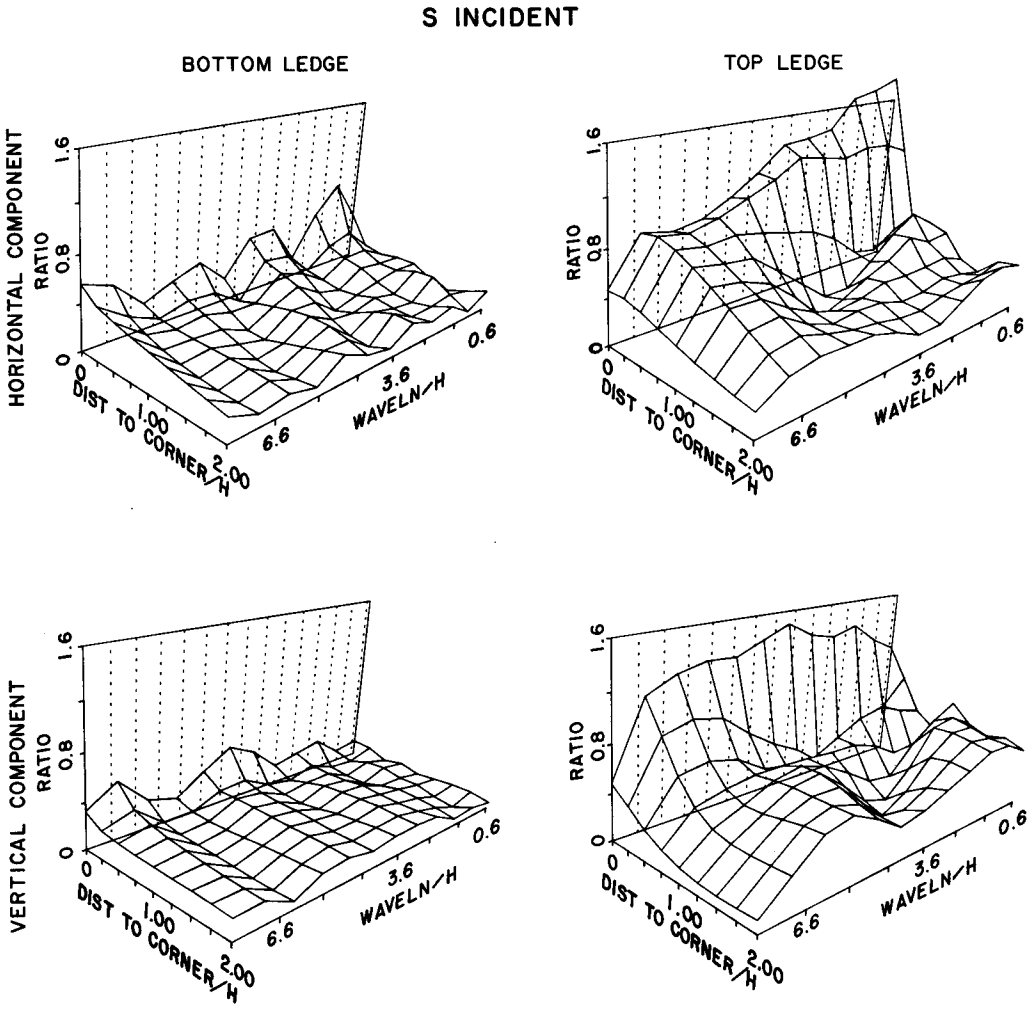

FIG. 6. Ratios of spectral amplitudes for S incident on a vertical step.

Figure 2 shows that the bottom corner is the most efficient scatterer of P waves. On the lower shelf are two sets of scattered P and Rayleigh waves of about equal amplitude and opposite polarity, produced by the incident P wave and the P wave traveling back down after being reflected at the upper surface. The amplitude of the scattered Rayleigh wave on the lower shelf is similar to that found in a model experiment described by Gangi and Wesson (1978) in which they measured scattering coefficients for P waves impinging at various angles of incidence on wedges of different angles (they cut wedges out of a circle of metal and put a transducer on the rim to generate P waves and a transducer on one of the wedge faces to record the scattered waves). They measured a scattering coefficient on the vertical component of 0.23, relative to the maximum P motion at the corner; we find a coefficient of 0.20 (Figure 4).

In contrast to scattering of incident P waves, the top corner is the most efficient scatterer for incident S waves (Figure 3). The scattering on the lower shelf from the lower corner is similar in character and amplitude to that from incident P waves,

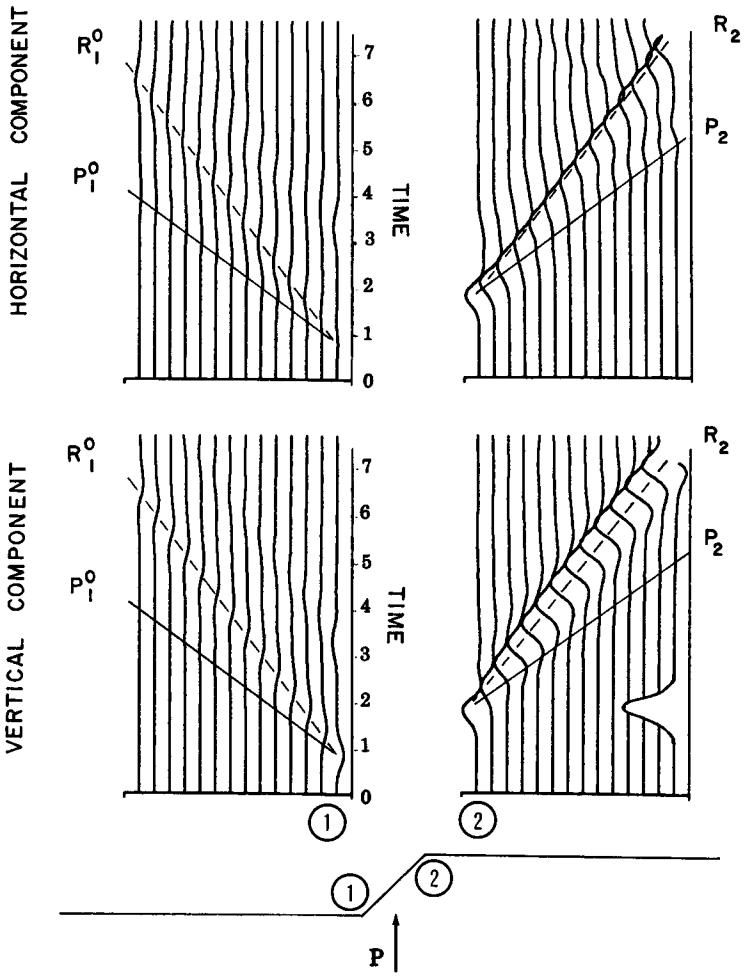

FIG. 7. Inclined step, *P* incident: scattered field time histories, with the reference motion added to the rightmost vertical trace. The small phase propagating to the *left* in the horizontal component, *top* seismograms is a numerical artifact from the *right edge* of the model; it is also seen in Figure 8. See Figure 2 legend for additional details.

but large amplitude Rayleigh waves, with an amplitude of about 0.45 of the reference wave, are scattered from the top corner.

The spectra do not add much to what can be inferred from the time histories (Figures 5 and 6). They are broadband and therefore, the levels are similar to time-domain scattering coefficients; modulation effects due to interaction of various phases are present. The spectra and time series both have anomalously large motions that are restricted to the region near the corners. Perhaps the most important finding is that the scattered field has significant amplitude for wavelengths many times the height of the step.

Inclined step. For incident *P* waves and an inclined step, the bottom corner is a less efficient scatterer than for the vertical step (compare Figures 7 and 2). The upper corner produces much larger surface waves traveling along the upper surface than for a step change in topography. Incident *S* waves produce scattered waves of similar amplitude for both inclined and vertical steps (Figure 8).

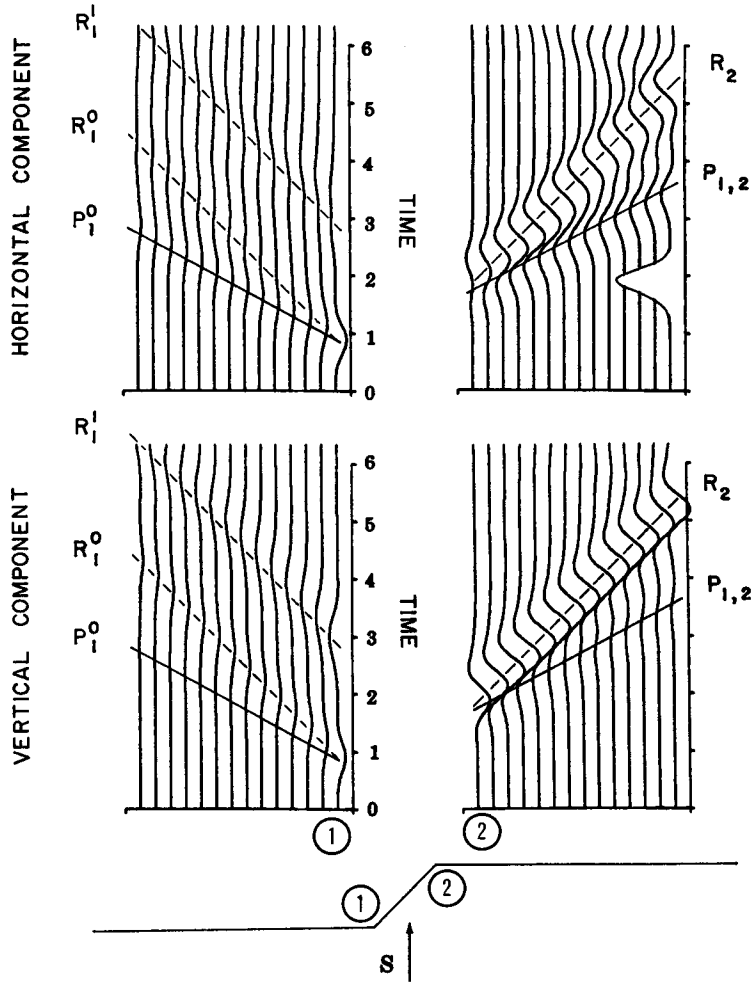

FIG. 8. Inclined step, S incident: scattered field time histories, with reference motion added to the rightmost horizontal trace. The phase labeled $P_{1,2}$ corresponds to a P wave traveling from corner 1 to corner 2, then horizontally away from corner 2. See Figure 2 legend for additional details.

DISCUSSION

It is easy to see qualitatively why the lower corner of the vertical step must act as a wave scatterer for vertically incident waves. Consider the vicinity of the lower corner: in the absence of any wave scattering, the motion in the interior (to the right of the step in Figure 1) would be half that on the lower shelf. This discontinuity in motion gives rise to the scattered waves (Gangi, 1967). The analysis for the upper corner is not as clear. The scattered waves depend on the relative amplitude, near the upper corner, of the motion along the vertical cliff face and nearby interior points. Why scattering from the upper corner produces large Rayleigh waves for an incident S wave but small ones for incident P waves is not clear. The relative increase in scattered Rayleigh waves along the upper shelf for incident P waves and the inclined step is undoubtedly produced in part by the reflection along the sloping surface of the incident wave into grazing angles.

The amplitudes of the scattered waves, especially the scattered Rayleigh waves

along the upper shelf due to incident S waves, are not negligible and may have a critical bearing on design in some specialized situations (e.g., a power-generating station near a sea cliff). Results for other angles of incidence and the model experiments of Gangi and Wesson (1978) suggest that the amplitude of the scattered waves is a weak function of angle around vertical incidence.

Acknowledgments

We thank D. J. Andrews and W. B. Joyner for critical reviews of the original manuscript, Leonard Bond for useful suggestions, and G. Wojcik for help in discovering a numerical error that plagued us for a long time.

References

Alterman, Z. S. and A. Rotenberg (1969). Seismic waves in a quarter plane, *Bull. Seism. Soc. Am.* **59,** 347–368.

Alterman, Z. S. and D. Loewenthal (1970). Seismic waves in a quarter and three-quarter plane, *Geophys. J.* **20,** 101–126.

Bond, L. J. (1979). A computer model of the interaction of acoustic surface waves with discontinuities, *Ultrasonics* **17,** 71–77.

Boore, D. M. (1972). Finite difference methods for seismic wave propagation in heterogeneous materials, in *Methods in Computational Physics*, vol. 11, B. A. Bolt, Editor, Academic Press, New York, pp. 1–37.

Bouchon, M. (1973). Effect of topography on surface motion, *Bull. Seism. Soc. Am.* **63,** 615–632.

Clayton, R. and B. Engquist (1977). Absorbing boundary conditions for acoustic and elastic wave equations, *Bull. Seism. Soc. Am.* **67,** 1529–1540.

Fuyuki, M. and Y. Matsumoto (1980). Finite difference analysis of Rayleigh wave scattering at a trench, *Bull. Seism. Soc. Am.* **70,** 2051–2069.

Gangi, A. F. (1967). Experimental determination of P wave/Rayleigh wave conversion coefficients at a stress-free wedge, *J. Geophys. Res.* **72,** 5685–5692.

Gangi, A. F. and R. L. Wesson (1978). P-wave to Rayleigh-wave conversion coefficients for wedge corners; model experiments, *J. Comp. Physics* **29,** 370–388.

Greenfield, R. J. (1971). Short-period P-wave generation by Rayleigh-wave scattering at Novaya Zemlya, *J. Geophys. Res.* **76,** 7988–8002.

Hudson, J. A. and D. M. Boore (1980). Comments on "scattered surface waves from a surface obstacle" by J. A. Hudson, *Geophys. J.* **60,** 123–127.

Ilan, A., A. Ungar, and Z. S. Alterman (1975). An improved representation of boundary conditions in finite difference schemes for seismological problems, *Geophys. J.* **43,** 727–742.

Ilan, A. and D. Loewenthal (1976). Instability of finite difference schemes due to boundary conditions in elastic media, *Geophys. Prospecting* **24,** 431–453.

Ilan, A., L. J. Bond, and M. Spivack (1979). Interaction of a compressional impulse with a slot normal to the surface of an elastic half space, *Geophys. J.* **57,** 463–477.

Key, F. A. (1967). Signal-generated noise recorded at the Eskdalemuir seismometer array station, *Bull. Seism. Soc. Am.* **57,** 27–37.

Key, F. A. (1968). Some observations and analyses of signal generated noise, *Geophys. J.* **15,** 377–392.

U.S. Geological Survey
345 Middlefield Road
Menlo Park, California 94025 (D.M.B.)

U.S. Geological Survey
Golden, Colorado 80225 (S.C.H., S.T.H.)

Manuscript received June 9, 1980